A novel two-degrees-of-freedom piezoelectric energy harvester

Wu, Hao; Tang, Lihua; Yang, Yaowen; Soh, Chee Kiong

A NOVEL 2-DOF PIEZOELECTRIC ENERGY HARVESTER

Hao WU[1], Lihua TANG[2], Yaowen YANG[3]*, CheeKiong SOH[4]

[1]School of Civil and Environmental Engineering, Nanyang Technological University
50 Nanyang Avenue, Singapore 639798
[3]* Corresponding author, cywyang@ntu.edu.sg; [1]hwu1@e.ntu.edu.sg
[2]lihuatang@pmail.ntu.edu.sg [4]csohck@ntu.edu.sg

Abstract

Energy harvesting from ambient vibrations using piezoelectric effect is a promising alternative solution for powering small electronics such as wireless sensors. A conventional piezoelectric energy harvester (PEH) usually consists of a cantilevered beam with a proof mass at its free end. For such a device, the second resonance of the PEH is usually ignored because of its high frequency as well as low response level compared to the first resonance. Hence, only the first mode has been frequently exploited for energy harvesting in the reported literature. In this paper, a novel compact PEH using two vibration modes has been developed. The harvester comprises one main cantilever beam and an inner secondary cantilever beam, each of which is bonded with piezoelectric transducers. By varying the proof masses, the first two resonant frequencies of the harvester can be tuned close enough to achieve useful wide bandwidth. Meanwhile, this compact design efficiently utilizes the cantilever beam by generating significant power output from both the main and secondary beams. Experiment and simulation have been carried out to validate the design concept. The results show that the proposed novel PEH is more adaptive and functional in practical vibrational circumstances.

Keywords: energy harvesting; vibration; 2 DOF system; broadband; resonant frequency

1. INTRODUCTION

With recent advancement in integrated circuits, energy consumption of micro-scale electronics like wireless sensors has been greatly reduced. Due to many limitations of powering such electronics by batteries, great research interests have been attracted to harvesting energy from the ambient environment to power these electronics. Among the different kinds of energy source existing in the environment, vibration sources is the most ubiquitous and can be found everywhere in our daily life. One promising option for vibration energy harvesting is using piezoelectric material.

Most PEHs work as linear vibration resonators, in which the system performance largely relies on the resonant frequency. A conventional PEH usually consists of a cantilever beam with a proof mass at its free end. For such a device, it mostly works at its first resonant frequency, while its high-order modes are usually neglected because they are far away and provide much lower response level as compared to the first mode. Thus, only the first mode of the PEH is exploited for energy harvesting and it is usually regarded as a Single-Degree-of-Freedom (SDOF) harvester. However the source of practical vibrations in the environment is usually frequency-variant or random with energy distributed over wide frequency range. Thus, a conventional PEH using only single mode is definitely inefficient. To overcome this limitation, many researchers have attempted to develop systems with the capability of broadband energy harvesting. A great number of approaches have been proposed for broadband vibration energy harvesting (Tang et al., 2010). These techniques can be categorized into multi-modal harvesting technique (Shahruz, 2006; Ferrari et al., 2008; Xue et al., 2008; Qi et al., 2010; Tadesse et al., 2009; Ou et al., 2012; Arafa et al., 2011; Erturk et al., 2009a; Kim et al., 2011), resonance tuning approach (Roundy and Zhang, 2005; Leland and Wright, 2006; Eichhorn et al., 2009), and non-linear technique (Cottone et al., 2009; Erturk et al., 2009b; Arrieta et al., 2010; Tang et al., 2012).

Various kinds of designs for multi-modal energy harvesting have been reported in the literature. Shahruz (2006), Ferrari et al. (2008) and Xue et al. (2008) proposed similar systems comprising an array of cantilevered energy harvesters with various lengths and tip masses. These cantilevers with different working frequencies can be carefully designed to cover certain range of frequency to achieve a broader bandwidth. Qi et al. (2010) also developed a different multi-resonance energy harvester by installing additional cantilever array to one beam. However, these designs significantly increase the volume and weight of the system, which not only sacrifices the power density but also limits its applicability. Rather than using the cantilever array configuration, some researchers have developed multiple-DOF energy harvesters based on one single beam. Tadesse et al. (2009) presented a design of multi-modal energy harvesting beam employing both electromagnetic and piezoelectric transduction mechanisms, each of which was efficient for a specific mode. Ou et al. (2012) presented a 2-DOF system by using a two-mass cantilever beam. Although two useful modes were obtained, the harvester cannot be regarded as true broadband as the two resonances were quite far away (at about 50 Hz and 350 Hz in their experiment study). Aldraihem et al. (2011) and Zhou et al. (2012) developed a 2-DOF harvester in which a dynamic magnifier was adopted. With the dynamic magnifier, the power output from the harvester was magnified, and multi-modal response was also presented in their study. However, it could not achieve two close working frequencies unless an impractical huge magnifier was employed. Erturk et al. (2009) developed a PEH with L-shaped beam configuration where the second natural frequency approximately doubled the first. Generally, the purpose for designing a broadband multi-modal energy harvester is to achieve close resonances with significant magnitudes for effective energy conversion, but most of the previous designs can only achieve resonances far away from each other with second peak much smaller than the first. Kim et al. (2011) developed a 2-DOF system that could achieve two close resonances by using both translational and rotational degrees of freedom of a vibration body, but this design required an additional vibration body to be attached to two cantilevers, which increased the volume as well as the complexity of the harvester.

In this paper, a novel compact 2-DOF energy harvester is developed aiming at achieving two close resonances with significant magnitudes. This harvester comprises one main cantilever and an inner secondary cantilever. It can be conveniently fabricated from a conventional SDOF harvester by cutting the inner beam inside and attaching an additional proof mass. This configuration is referred to as "cut-out" beam hereafter. By using this design, without increase of volume, the first two close resonances with significant magnitudes can be obtained. Experiment and simulation are performed to prove this concept.

2. COMPARISON OF 2-DOF CANTILEVER PEHs

Conventionally, a 2-DOF cantilever PEH comprises a continuous beam and 2 proof masses, as shown in Figure 1(a). Although such design produces two resonances, the second resonant frequency is about several times larger than the first when L_1 is equal to L_2 and the weights of two masses are the same as shown in Figure 1(b). Even if the two resonant frequencies can be tuned by adjusting the length and weight of tip masses, they cannot be tuned very close to each other.
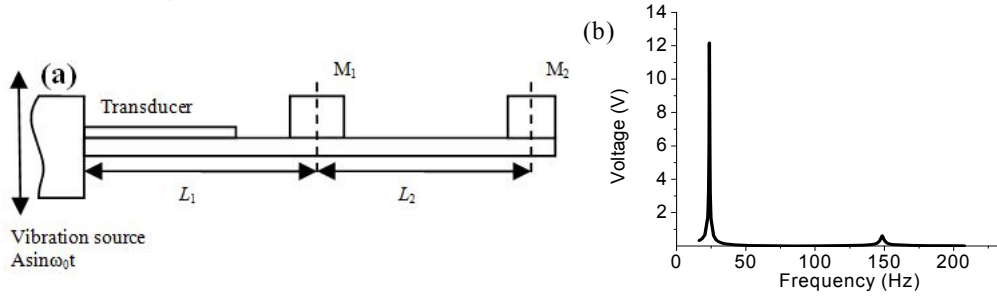

Figure 1. (a) A conventional 2-DOF cantilever PEH (b) typical frequency response

The fundamental difference between our proposed harvester and the conventional 2-DOF harvester is that the secondary beam (L_2) is cut inside the main beam (L_1) rather than extended outwards from the main beam. This geometric discrepancy results in difference in the stiffness matrix of the proposed and conventional 2-DOF harvesters. To illustrate this point, we compared the simplified cut-out cantilever beam model (our design) with the continuous cantilever beam model (other's design), as shown in Figure 2.
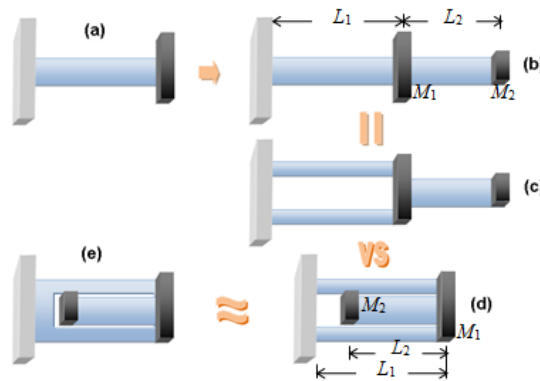

Figure 2. Comparison of (a) SDOF cantilever, (b) conventional continuous cantilever, (c) equivalent continuous cantilever, (d) simplified cut-out cantilever and (e) actual cut-out cantilever

The primary cantilever beam (length L_1) in the cut-out configuration (Figure 2(d)) is assumed to have the same elastic modulus, thickness and overall width as the secondary beam (length L_2). Thus, the flexural rigidity EI is uniform throughout. This assumption also applies to the conventional continuous configuration in Figure 2(c). Although there is slight difference between the simplified

model and the actual model in the experiment due to the different width at the root of main beam, it can be neglected as we only use the simplified model to illustrate the difference of natural frequencies between cut-out configuration and continuous configuration. Both configurations can be modeled as the lumped parameter system by neglecting the distributed mass of the cantilever beam. The mass matrices are the same for both:

$$[M] = \begin{bmatrix} M_1 & 0 \\ 0 & M_2 \end{bmatrix} = M_1 \begin{bmatrix} 1 & 0 \\ 0 & \alpha \end{bmatrix} \tag{1}$$

The difference in stiffness matrices is the key that two configurations generate different frequency responses. The stiffness matrix for the cut-out beam configuration is:

$$[K]_a = \frac{6EI}{(3\beta^2 + 4\beta^3)L_1^3} \begin{bmatrix} 2 - 6\beta + 6\beta^2 + 2\beta^3 & 3\beta - 2 \\ 3\beta - 2 & 2 \end{bmatrix} \tag{2}$$

While the stiffness matrix of the conventional continuous beam configuration is:

$$[K]_b = \frac{6EI}{(3\beta^2 + 4\beta^3)L_1^3} \begin{bmatrix} 2(1+\beta)^3 & -3\beta - 2 \\ -3\beta - 2 & 2 \end{bmatrix} \tag{3}$$

where the non-dimensional parameter α denotes the proof mass ratio of M_2/M_1, and β denotes the ratio of L_2/L_1. Solving the eigenvalue problem of the two configurations, we can obtain two roots of ω^2 where ω is the natural frequency. The non-dimensional difference of the two roots of the eigenvalue problem can be given as,

$$\frac{\Delta(\omega^2)^a}{\omega_s^2} = \frac{4\sqrt{[\alpha(1 - 3\beta + 3\beta^2 + \beta^3) + 1]^2 - \alpha(3\beta^2 + 4\beta^3)}}{\alpha(3\beta^2 + 4\beta^3)} \tag{4}$$

$$\frac{\Delta(\omega^2)^b}{\omega_s^2} = \frac{4\sqrt{[\alpha(1 + 3\beta + 3\beta^2 + \beta^3) + 1]^2 - \alpha(3\beta^2 + 4\beta^3)}}{\alpha(3\beta^2 + 4\beta^3)} \tag{5}$$

Where ω_s denotes the natural frequency of the SDOF cantilever beam with length L_1 and proof mass M_1. Note that the only difference in the above equations is that the term 3β has opposite sign. For both configurations, when α approaches zero, two resonant frequencies approach each other. But this means that the mass for the secondary beam decreases to zero, making the system degrade to a SDOF system, which is of no interest. Other than that, the cut-out cantilever beam can also achieve two equal resonant frequencies when β→ 2/3 and α→ 27/17 by taking derivative of Eqn. (4). However, for the continuous beam, it is not possible to obtain two close resonances from Eqn. (5) with non-zero α. This unique property of the cut-out cantilever configuration provides a practical parametric option to implement a 2-DOF energy harvester with two close resonances.

3. EXPERIMENTAL STUDY

Based on the cut-out cantilever concept, we devise a 2-DOF cut-out harvester as well as a conventional SDOF harvester for comparison. Experiment is performed to compare the two harvesters and to show the advantage of this novel design. As stated in section 2, we use a simplified model to illustrate the concept of 2-DOF cut-out beam and that simplified model neglects the non-uniform stiffness and the distributed mass of the beam. Thus it cannot be directly used as a guide to design the parameter for the 2-DOF cut-out configuration. A rough finite element analysis (FEA) simulation for determining the parameters and the natural frequencies of the 2-DOF beam is done before the experiment. After the experiment, more simulation works are done to validate the experimental results. The detailed simulation work is discussed in section 4.

3.1 Experiment setup

Figure 3 shows the fabricated prototypes installed on a vertical seismic shaker. The detailed dimensions of the two harvesters are shown in Figure 4.
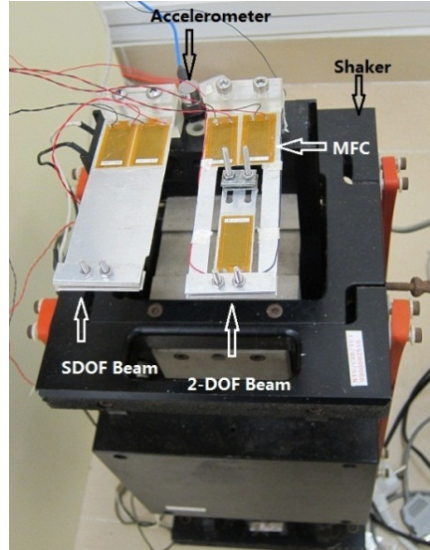
Figure 3. Conventional SDOF and proposed 2-DOF cut-out harvesters installed on seismic shaker.
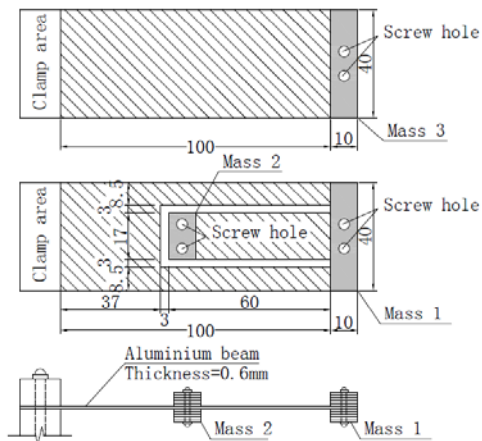

Figure 4. Geometry of conventional SDOF and proposed 2-DOF harvesters, (All dimensions in mm).

The SDOF cantilever beam and the 2-DOF cut-out cantilever beam are both made from pieces of aluminum plates (110mm*40mm*0.6mm). Specially, the cut-out 2-DOF cantilever beam is fabricated by cutting inside of the SDOF one. Pieces of steel are screwed at the free end of the beams in the experiment, such that the weight of the proof masses can be adjusted conveniently. Besides, MFC sheets (M-2814-P2, by Smart Material Corp.) with d_{31} piezoelectric effect are used for vibration-to-electricity transduction. Two pieces of MFC sheets are bonded at the root of the main beam, while another one piece bonded at the root of the secondary beam. For comparison, the conventional SDOF harvester also has 2 pieces of MFC sheets at its beam root.

The schematic of the whole experiment setup is shown in Figure 5. The harmonic excitation signal is generated by the function generator, adjusted by the power amplifier and finally fed to the seismic shaker. In the experiment, the excitation frequency is manually swept from 10 Hz to 30 Hz. During this sweeping procedure, the excitation acceleration is monitored by an acceleration data logger as feedback loop and controlled at 1m/s². The open circuit voltage outputs generated by the MFC sheets are logged by the digital multimeter.
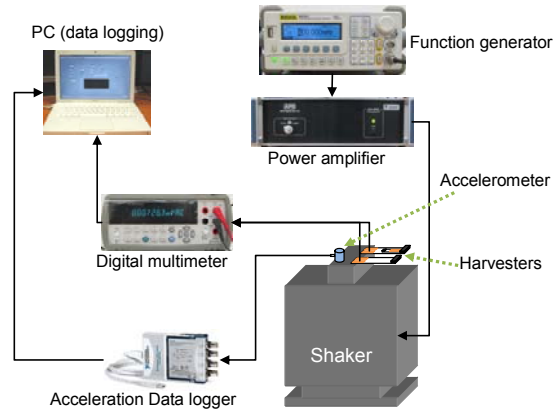
Figure5. Schematic of the experiment setup.

3.2 Open circuit voltage response

The open circuit voltage responses are recorded from both the main beam and the secondary beam. The weight of the secondary mass M_2 is varied in the experiment; and the results are shown in Figure 6.
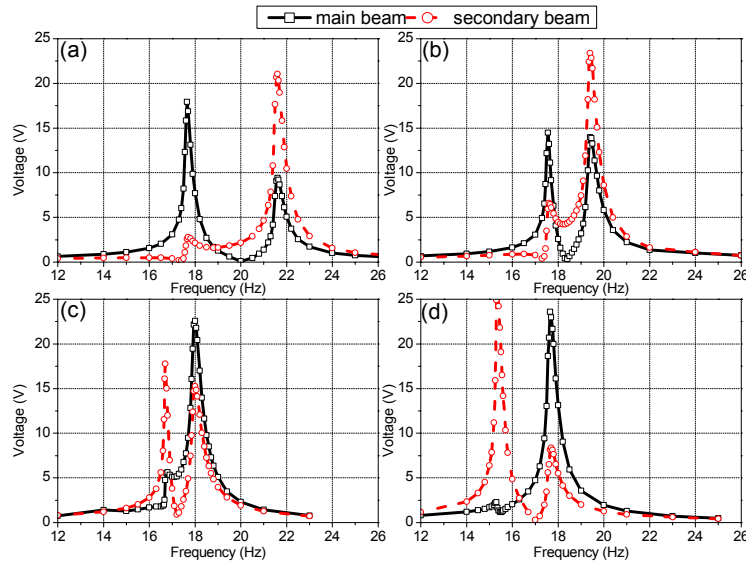

Figure 6. Measured open circuit voltage output with different secondary mass when M_1=7.2g. (a) M_2=8.8g, (b) M_2=11.2g, (c) M_2=14.2g and (d) M_2=16.8g.

As shown in Figure 6, different frequency responses are obtained when M_2 is varied from 8.8g to 16.8g while keeping M_1=7.2g. When M_2=8.8g, the two resonance peaks obtained are 17.5Hz and 21.6Hz.The voltage output from the main beam is higher at the first resonance than that at the second while the voltage output from the secondary beam voltage is just on the contrary. When M_2 increased to 11.2g (Figure 6(b)), the two resonances are quite close to each other (17.4Hz and 19.6Hz), and the amplitudes of the two peaks of main beam voltage are almost equal. Although the amplitudes are slightly smaller than the first resonance peak in Figure 6(a), the two resonance frequencies are much closer, which will benefit energy harvesting from a given continuous working frequency range. However, in this case, the secondary beam did not provide two equal peaks in voltage response. When M_2=14.2g (Figure 6(c)), the two resonance frequencies are 16.8Hz and 18.0Hz, and the two equal peaks appeared in the voltage response of the secondary beam while the two peaks in the response

from main beam is not equal. As M_2 further increased, different from Figure 6(a), a reverse trend of voltage response is observed in Figure 6(d).

Meanwhile, the open circuit voltage response of SDOF cantilever beam for different tip masses are also obtained in the experiment, as shown in Figure 7.
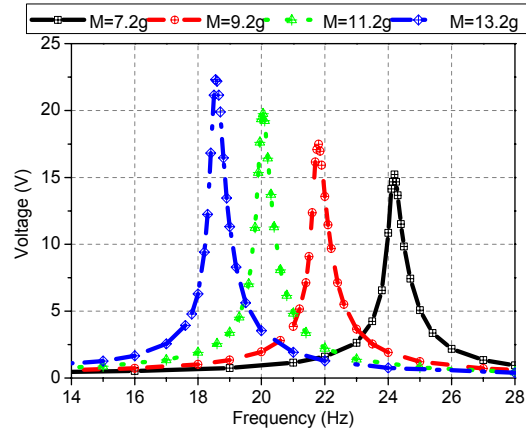

Figure 7. Measured open circuit voltage output for SDOF harvester
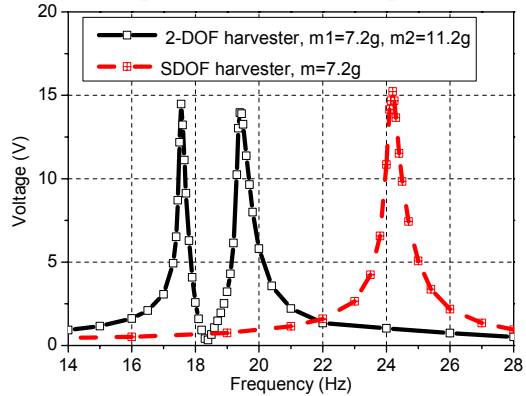

Figure 8. Comparison of open circuit voltage responses

Figure 8 compares the open circuit voltage responses of the cut-out 2-DOF harvester and the conventional SDOF harvester. The tip masses on the main beam of the cut-out 2-DOF cantilever and on the SDOF beam are both 7.2g.The tip mass on the secondary beam of the cut-out cantilever is M_2=11.2g. It is obvious that the 2-DOF configuration has two close peaks with the same magnitude as that of the SDOF configuration (about 15V). But the cut-out 2-DOF configuration has significantly wider bandwidth than the conventional SDOF harvester. As shown in Figure 8, the bandwidth in the open circuit voltage spectrum at voltage level of 3V for the cut-out 2-DOF harvester is about 3.0 Hz (by adding up the two segments near the two resonances), which is much more advantageous over the 2.1Hz of the SDOF harvester.

Other than the broader bandwidth achieved by the cut-out 2-DOF configuration, the proposed cut-out design can also fully utilize the cantilever beam for harvesting energy. Conventionally, the area of the secondary beam is not used or used inefficiently because of the low voltage output (due to low strain level near free end) in the SDOF cantilever beam configuration. But in this cut-out configuration, by adjusting the tip masses, the response level of the secondary beam can also be tuned to be comparable with that of the main beam, as shown in Figure 6. Thus the secondary beam can also have significant contribution to energy harvesting.

3.3 Power output response

Other than the open circuit voltage response, power output response is also a concern in evaluating the performance of an energy harvester. A resistor is usually connected to the harvester as an electrical load. To obtain the maximum power output from a harvester, the optimal resistor value should be determined according to impedance matching technique. In our experiment, a variable resistor ranging from 1kΩ to 999kΩ is connected to the SDOF and the 2-DOF cut-out harvesters to study their performance with different resistances. The exact optimal resistor values vary at each frequency point. However, the peak values around the resonance frequencies are of most interest to the research of power output from an energy harvester. Thus, for simplicity, rather than finding out every optimal resistor value at each frequency, we focused on the optimal resistor at the resonances because the responses at off-resonance frequencies are much lower. An approximate value of optimal resistor should be chosen for further study. Figure 9 shows the frequency response of the power output with different resistor values for the main beam of the 2-DOF cut-out harvester when M_1=7.2g and M_2=8.8g. It can be observed that when the resistor value is around 120kΩ, the harvester has a maximum response for power output, for both two peaks.

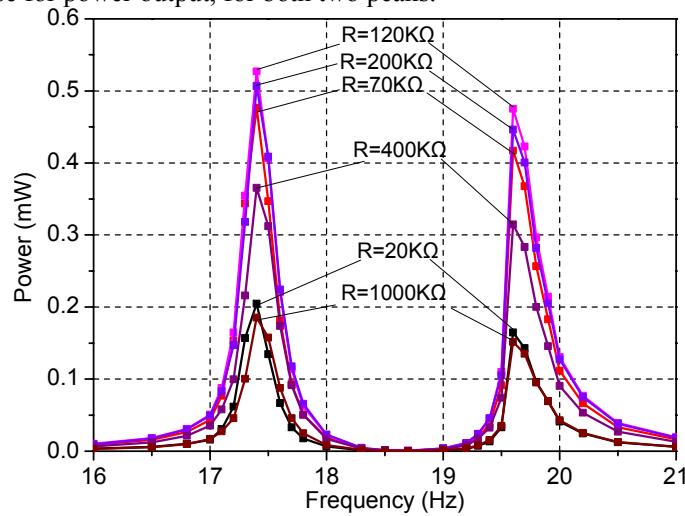**Figure 9.** Experimental results of frequency response of the power output for the main beam of the 2-DOF cut-out beam when M_1=7.2g and M_2=8.8g.
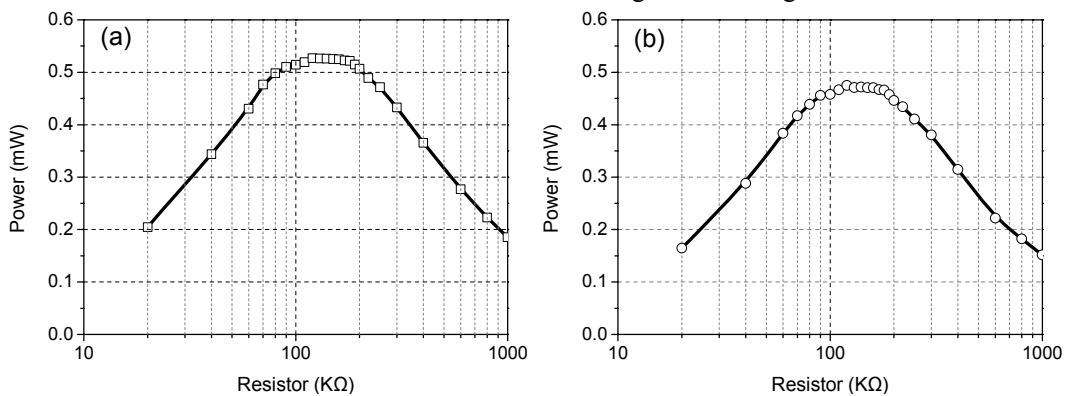

Figure10. Measured power output versus resistor value for the main beam of the 2-DOF cut-out beam when M_1=7.2g and M_2=8.8g at (a) 1st resonant frequency 17.4 Hz (b) 2nd resonant frequency 19.6 Hz.

Figure 10 illustrates more clearly the power output from the main beam of the 2-DOF harvester versus the resistor value at 17.4 Hz and 19.6 Hz (two resonant frequencies obtained in the open circuit condition). It is noted that the optimal resistor value which can be determined is located in the range from about 120 to 160kΩ for both resonances. In such a range, the maximum power output does not vary so much. Therefore, by choosing a resistor value in the range, the frequency response for optimal

power output can be obtained. Although this value is not the exact value for optimization at each frequency, the error by using this is quite small especially when the frequency range is quite near the resonance.
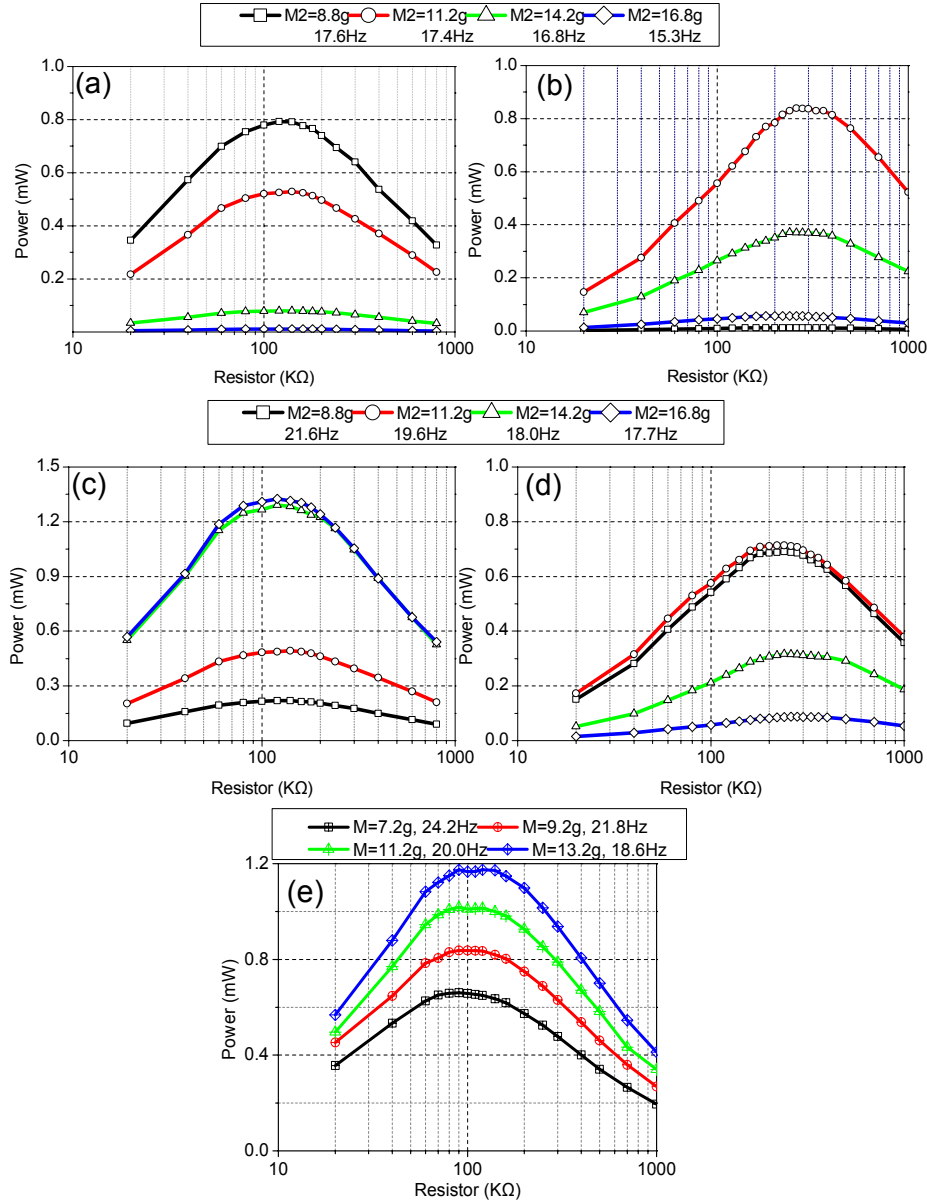

Figure 11. Optimal power output of (a) main beam and (b) secondary beam of cut-out harvester at first resonance; (c) main beam and (d) secondary beam of cut-out harvester at second resonance; and (e) SDOF harvester at its resonance.

More results of the optimal power and its corresponding optimal resistor value for both the main beam and the secondary beam with different configuration of the 2-DOF cut-out harvester as well as the SDOF harvester are given in Figure 11. The power output responses versus resistor values for four configurations with different proof masses are studied at their resonant frequencies obtained from the open circuit condition. From these results, even with different configurations, the optimal resistor value for the main beam of the 2-DOF cut-out harvester all located in the similar range, thus the value $R_1 = 130 k\Omega$ is chosen for later use. For the secondary beam, the optimal resistor value of $R_2 = 250 k\Omega$ is chosen. For the SDOF harvester, it is almost the same as the main beam of the 2-DOF harvester, $R = 130 k\Omega$. By using these optimal resistor values, we generate the maximum power output from these

harvesters connected with simple resistor as the electrical load, $P=U^2/R$. The results for different configurations are shown in Figure 12.
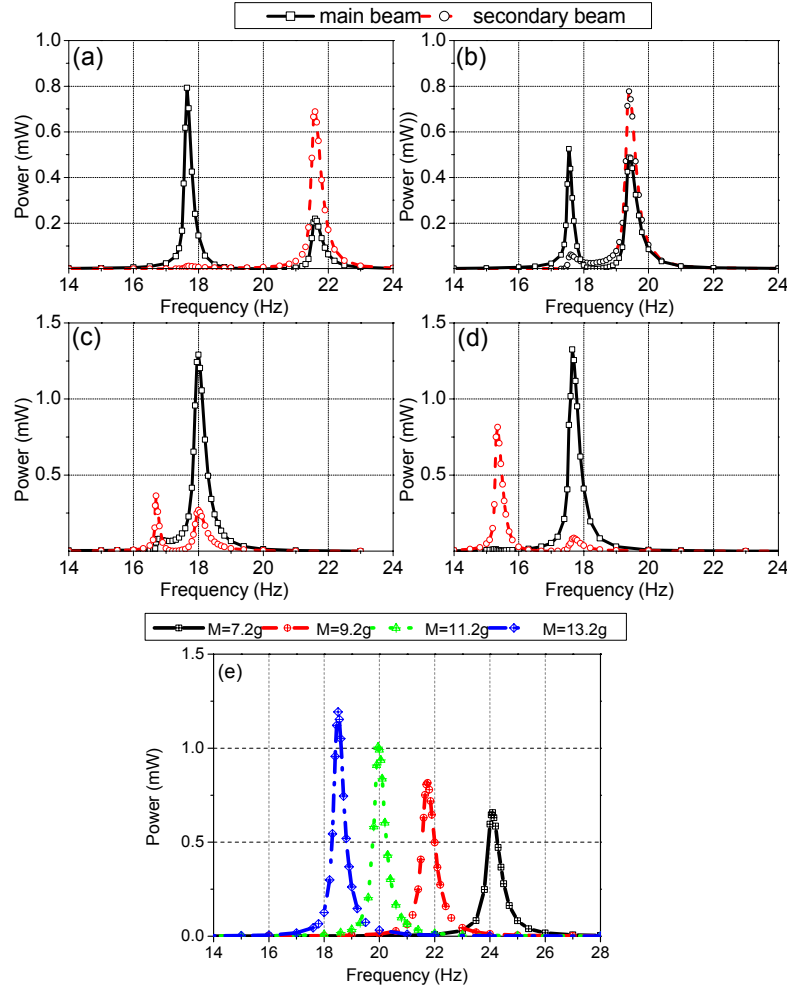

Figure 12. Experimental results of maximum power output for 2-DOF cut-out harvester for $R_1=130k\Omega$ and $R_2=250k\Omega$ when $M_1=7.2g$, (a) $M_2=8.8g$, (b) $M_2=11.2g$, (c) $M_2=14.2g$, (d) $M_2=16.8g$, and for (e) SDOF harvester (R=130kΩ)

Figure 12 show that both the MFC transducers on the main and secondary beams can generate significant power output when tip masses are properly selected. It is noted that the best overall power output (power outputs from both the main and secondary beams) may not occur when the two resonances are very close (Figure 12(c)). In such case, only one peak in the response of the main beam can significantly contribute to energy harvesting and the contribution from the secondary beam is negligible, which cannot be regarded as an efficient design in terms of bandwidth. Instead, when $M_2=8.8g$ or 16.8g, although the two resonances are slightly further away, both the main and secondary beams have one significant peak. Thus the cut-out harvester has significant overall power output at both resonant frequencies and broadband energy harvesting is achieved. To achieve this, the detailed parameters of the 2–DOF cut-out configuration should be carefully designed. Compared to the SDOF harvester with M=7.2g, the peaks of the cut-out harvester can have larger magnitudes (e.g., Figures 12(c) and 12(d)). For an increased tip mass M=13.2g for SDOF harvester, the peak magnitude of the SDOF harvester is comparable with that of the cut-out harvester. However, the cut-out harvester is still advantageous in terms of bandwidth.

In conclusion, the cut-out 2-DOF harvester proposed in this paper can achieve not only broader bandwidth, but also greater power outputs as compared to the SDOF harvester by fully utilizing the cantilever beam.

4. VALIDATION USING FEA NUMERICAL SIMULATION

Numerical simulation using Finite Element Analysis (FEA) is carried out to validate the experimental findings.

4.1 Modeling of harvester

The finite element model of the cut-out beam is implemented in the commercial FEA software ANSYS. ANSYS provides a unique element (SOLID 226 element) for coupled-field analysis which can be used to model the piezoelectric transducers. Conventional SOLID 186 element is used to model the aluminum substrate of beams and tip masses. The load resistor connected to the piezoelectric transducers is modeled using the CIRCU 94 element. The degree of freedoms of electrical potential of the nodes on the top and bottom surfaces of the piezoelectric transducers are coupled respectively to achieve the uniform electrical potential on electrodes, and then connected to the two terminals of the load resistor. Two resistors are connected to the two transducers on the main and secondary beams separately. Thus, the FEA model of the piezoelectric energy harvester connected with resistors is established. Modal analysis is performed to determine the first two vibration modes and steady state analysis is performed to obtain the voltage responses from the harvester. The dimensions in the FEA model are set according to the devised prototype.

The first two vibration modes are predicted by modal analysis, as shown in the Figure 13. In this case, M_1=7.2g, and M_2=8.8g. The resonant frequencies obtained from simulation are almost consistent with the experimental results (17.5Hz and 21.6Hz). Although they are not shown here, for the other cases, the predictions of natural frequencies are also consistent with the experimental results.
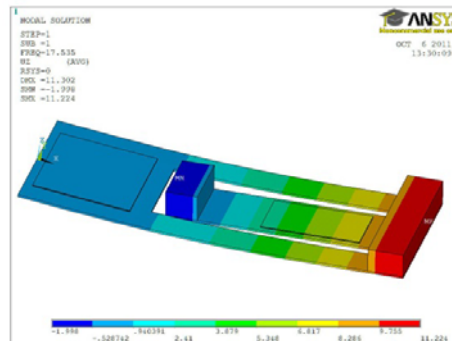
(a) First mode, resonant frequency=17.5Hz
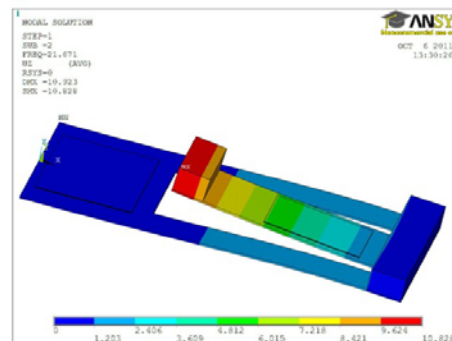
(b) Second mode, resonant frequency=21.7Hz

Figure 13. First and second modal shapes of cut-out harvester

4.2 Steady-state analysis for open circuit voltage output

Other than modal analysis, the steady-state open circuit voltage response of the proposed harvester can also be obtained by harmonic analysis in ANSYS. By setting the resistor extremely large, the harvester can be regarded as in open circuit condition (i.e., the voltage obtained from the resistor in harmonic analysis is open circuit voltage response). Prior to the harmonic analysis, the damping ratios are measured using the attenuation curves obtained in the experiment at two resonant frequencies. As the resonant frequency only shifts around 20 Hz, the difference of damping ratio in this small frequency range is minor, and the damping ratio measured in different groups of tests varies around 0.65%~0.75%. Therefore, the overall structural damping ratio is simply set as a constant damping ratio of 0.7% in the harmonic analysis instead of Rayleigh damping.
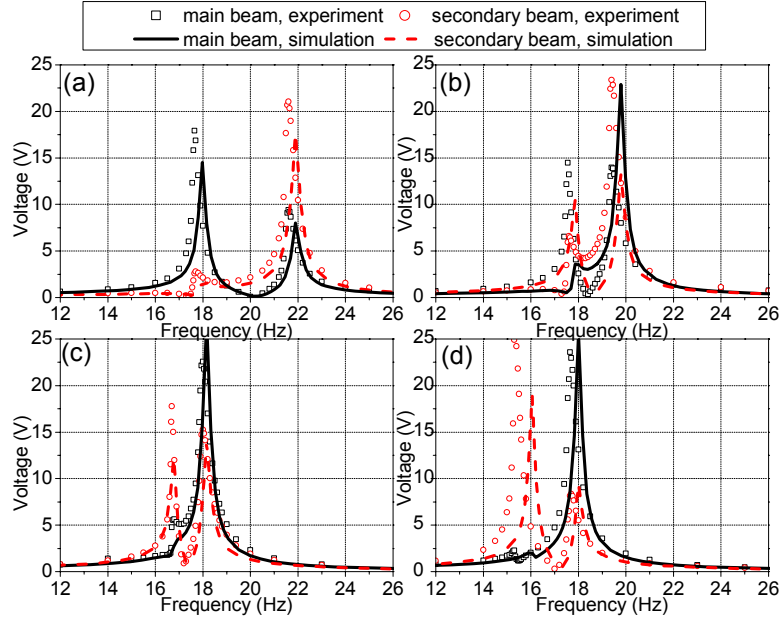

Figure 14. Comparison of simulation and experiment results for open circuit response with different second mass when M_1=7.2g. (a) M_2=8.8g, (b) M_2=11.2g, (c) M_2=14.2g and (d) M_2=16.8g.

Figure 14 compares the predicted open circuit voltage responses from the numerical simulation with the experimental results. Although there are small discrepancies in resonances and magnitudes, in general the simulation results agree well with the experimental ones. The simulation results also well indicate the trends of the responses with the change of the tip mass.

4.2 Steady-state analysis for power output

By setting different values of the resistor, different power responses at various frequencies can be obtained, which can be compared with the experimental results. The simulation results shown in Figure 15 are obtained from the similar configuration as that for Figure 9, i.e., M_1=7.2g and M_2=8.8g. Comparing Figures 9 and 15, it is apparent that the simulation results are similar to the experimental ones except the slight shift of resonance frequencies and magnitudes of the peak power. Furthermore, Figure 15 also indicates that the optimal resistor value is around 120kΩ, consistent with the experimental results. Hence the same value of R_1=130KΩ is used for the resistor connected to the main beam to calculate the maximum power output. For the secondary beam, similar results are obtained and R_2=250kΩ is adopted as the optimal resistor value. In Figure 16, the power output responses versus frequency are worked out by using these resistor values. Again, these results are

similar to the experimental ones shown in Figure 12 with minor differences in resonant frequencies and magnitudes.
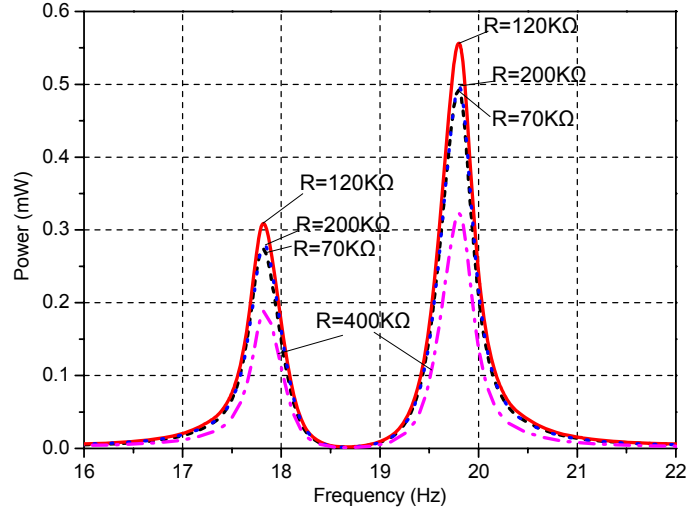

Figure 15. Simulation results of power output response versus frequency for the main beam of the 2-DOF cut-out beam when M_1=7.2g and M_2=8.8g.
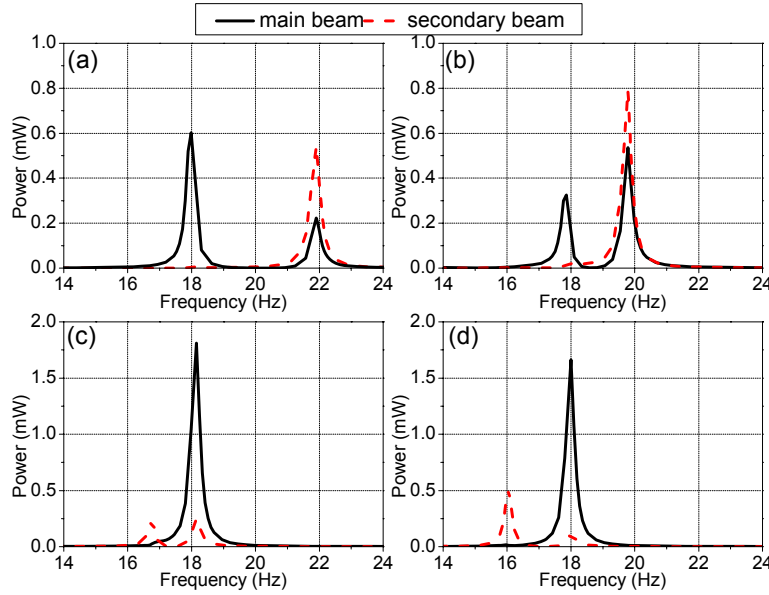

Figure 16. Simulation results of power output for 2-DOF cut-out harvester for R_1=130kΩ and R_2=230kΩ when M_1=7.2g (a) M_2=8.8g, (b) M_2=11.2g, (c) M_2=14.2g and (d) M_2=16.8g

Overall, these simulation results suggest that numerical simulation can be employed as a useful tool to provide guidelines for the design of 2-DOF cut-out harvester.

5. CONCLUSION

This paper proposed a novel design of 2-DOF cut-out cantilever PEH, which provides larger bandwidth compared to the conventional SDOF and 2-DOF PEHs. Meanwhile the proposed harvester is more compact than the conventional 2-DOF harvesters. It efficiently utilizes the material of cantilever beam by generating significant power output from both the main and secondary beams. With different proof masses, the open circuit voltage and the power output responses with resistive loads connected to the harvester have been studied in experiment. Subsequently, finite element

simulation has been conducted to validate the experiment results. The development of this novel 2-DOF cut-out harvester provides a new idea for designing a broadband multimodal energy harvester. Such design concept is useful in practice, especially when space constraint exists in real applications, such as micro-electro-mechanical systems.

References

1.   Aldrarihem, O., and Baz, A. 2011 "Energy Harvester with a Dynamic Magnifier" *Journal of Intelligent Material Systems and Structures*, 22, 521-530.

2.   Arrieta A. F., Hagedorn, P., Erturk, A. and Inman, D.J. 2010. "A piezoelectric bistable plate for nonlinear broadband energy harvesting" *Applied Physics Letters*, 97, 104102.

3.   Cottone, F., Vocca, H. and Gammaitoni, L. 2009. ''Nonlinear EnergyHarvesting,'' *Physical Review Letter*, 102, 080601.

4.   Eichhorn C, Goldschmidtboeing F and Woias P 2009. ''Bidirectional frequency tuning of a piezoelectric energy converter based on a cantilever beam"*Journal of Micromechanics and Microengineering*. 19, 094006.

5.   Erturk, A., Hoffmann, J. and Inman, D.J. 2009. "A Piezomagnetoelastic Structure for Broadband Vibration Energy Harvesting'' *Applied Physics Letters*, 94, 254102.

6.   Erturk A., Renno J. M., and Inman D. J. 2009 "Modeling of Piezoelectric Energy Harvesting from an L-shaped Beam mass Structure with an Application to UAVs", *Journal of Intelligent Material Systems and Structures*, 20, 529-544.

7.   Ferrari, M., Ferrari, V., Guizzetti, M., Marioli, D. and Taroni, A. 2008. ''Piezoelectric Multifrequency Energy Converter Power Harvesting in Autonomous Micro Systems,'' *Sensors and Actuators A*, 142, 329-335.

8.   Kim, I. H., Jung, H. J., Lee, B.M., and Jang, S. J. 2011 "Broadband energy-harvesting using a two degree-of-freedom vibrating body" *Applied Physics Letters,* 98, 214102.

9.   Leland, E.S. and Wright, P.K. 2006. ''Resonance Tuning of Piezoelectric Vibration Energy Scavenging Generators Using Compressive Axial Preload,'' *Smart Materials and Structures*, 15, 1413-1420.

10.   Ou, Q., Chen, X., Gutschmidt, S., Wood, A., Leigh, N. and Arrieta, A. F. 2012 "An experimentally validated double-mass piezoelectric cantilever model for broadband vibration-based energy harvesting" *Journal of Intelligent Material Systems and Structures* 23, 117-125.

11.   Qi S, Shuttleworth R, Olutunde O S and Wright J 2010 "Design of a multiresonant beam for broadband piezoelectric energy harvesting" *Smart Materials and Structures* 19, 094009.

12.   Roundy, S. and Zhang, Y. 2005. ''Toward Self-tuning Adaptive Vibration Based Micro-generators,'' *Proceedings of the SPIE*, 5649, 373-384.

13.   Shahruz, S. 2006. "Design of Mechanical Band-Pass Filters for Energy Scavenging" *Journal of Sound and Vibration*. 292, 987-998.

14.   Tadesse, Y., Zhang, S. and Priya, S. 2009. ''Multimodal Energy Harvesting Systems: Piezoelectric and Electromagnetic,''*Journal of Intelligent Material Systems and Structures*, 20, 625-632.

15.   Tang, L., Yang, Y., and Soh, C. K. 2010. "Toward Broadband Vibration-based Energy Harvesting," *Journal of Intelligent Material Systems and Structures*, 21, 1867-97.

16.   Tang, L., Yang, Y. and Soh, C.K. 2012. "Improving Functionality of Vibration Energy Harvesters Using Magnets," *Journal of Intelligent Material Systems and Structures* (in press).

17.   Xue H, Hu Y and Wang Q M 2008 "Broadband piezoelectricenergy harvesting devices using multiple bimorphs with different operating frequencies" *IEEE Transaction on Ultrasonic, Ferroelectrics and Frequency Control* 55 2014–8.

18.   Zhou, W., Penamalli, G. R. and Zuo L. 2012. "An efficient vibration energy harvester with a multi-mode dynamic magnifier" *Smart Materials and Structures* 21, 015014.